Title

Label-Free and Direct Visualization of Multivalent Binding of Bone Morphogenetic Protein-2 with Cartilage Oligomeric Matrix Protein

Journal

The Journal of Physical Chemistry B, 123(1)

ISSN

1520-6106

Authors

Tran, Victoria
Karsai, Arpad
Fong, Michael C
et al.

Publication Date

2019-01-10

DOI

10.1021/acs.jpcb.8b08564

Peer reviewed

Label-Free and Direct Visualization of Multivalent Binding of Bone Morphogenetic Protein-2 with Cartilage Oligomeric Matrix Protein

Victoria Tran,[1] Arpad Karsai,[1] Michael C. Fong,[2] Weiliang Cai[3] Jasper H.N. Yik,[3] Eric Klineberg,[3] Dominik R. Haudenschild,[3*] Gang-yu Liu[1*]

[1]Department of Chemistry, University of California, Davis, CA, 95616, United States

[2]Department of Biomedical Engineering, University of California, Davis, CA, 95616, United States

[3]Department of Orthopaedic Surgery, University of California-Davis Medical Center, Sacramento, CA, 95817, United States

*** Authors to whom correspondence should be addressed**

Dominik R. Haudenschild, Ph.D.
University of California, Davis
Department of Orthopaedic Surgery,
Sacramento, CA 95817
Phone: (916) 734-5015
Email: drhaudenschild@ucdavis.edu

Gang-yu Liu, Ph.D.
University of California, Davis
Department of Chemistry
Davis, CA 95616
Phone : (530) 754-9678
Fax : (530) 754-8557
Email: gyliu@ucdavis.edu

ABSTRACT: This work presents the first direct evidence of multivalent binding between bone morphogenetic protein-2 (BMP-2) and cartilage oligomeric matrix protein (COMP) using high-resolution atomic force microscopy (AFM) imaging. AFM topographic images reveal the molecular morphology of COMP, a pentameric protein whose five identical monomer units bundle together at N-termini, extending out with flexible chains to C-termini. Upon addition of BMP-2, COMP molecules undergo conformational changes at the C-termini to enable binding with BMP-2 molecules. AFM enables local structural changes of COMP to be revealed upon binding various numbers, 1-5, of BMP-2 molecules. These BMP-2/COMP complexes exhibit very different morphologies from those of COMP: much more compact and thus less flexible. These molecular level insights deepen current understanding of the mechanism of how BMP-2/COMP complex enhances osteogenesis among osteoprogenitor cells: i.e., multivalent presentation of BMP-2 via the stable and relatively rigid BMP-2/COMP complex could form a lattice of interaction between multiple BMP-2 and BMP-2 receptors. These ligand-receptor clusters lead to fast initiation and sustained activation of the Smad signaling pathway, resulting in enhanced osteogenesis. This work is also of translational importance, as the outcome may enable usage of lower BMP-2 dosage for bone repair and regeneration.

1. INTRODUCTION

Bone morphogenetic protein-2 (BMP-2), a member of the transforming growth factor beta (TGF-β) superfamily, plays an important role in bone repair and regeneration by inducing osteogenic differentiation of osteoprogenitor cells such as mesenchymal stem cells.[1-3] Whereas endogenous BMPs are active at the nanogram level, supraphysiological doses of BMPs are required to induce adequate bone formation clinically. This high dosage may cause significant side effects, and limits its therapeutic potential.[3-4] One established strategy to enhancing BMP-2's osteogenic effect is the reconstitution of the growth factor with extracellular matrix (ECM) components.[3, 5-6] Our prior investigations found that cartilage oligomeric matrix protein (COMP), when mixed with BMP-2, enhanced BMP-2-induced osteogenesis to a greater extent than BMP-2 alone, both in vitro and in vivo.[3, 7] The sustained presence of BMP-2 receptors, and sustained activation of Smad1/5/8 signaling were proposed as the possible mechanisms at cellular level.[3] To fully harness the therapeutic potential of BMP-2 and gain better understanding of enhancement mechanisms, molecular level knowledge of interactions between BMP-2 and matrix components such as COMP becomes essential, as the presentation of BMP-2 to cells is determined by the BMP-2 molecules residing in the individual BMP-2/COMP complexes.

This work utilizes high-resolution imaging of COMP, BMP-2 and mixtures of both components via atomic force microscopy (AFM). AFM was selected over x-ray crystallography because the latter provides spatially averaged structural information, and requires crystallization of proteins, which were proven challenging for BMP-2/COMP complexes. Unlike electron microscopy, which can capture two-dimensional projection, AFM can provide a three-dimensional topographical profile of the proteins. In principle, AFM can also be used to obtain high-resolution images of hydrated and live sample and monitor protein-protein in situ and in real time.[8-9] In

addition, unlike other imaging technologies which often require metal coating[10] or cryogenic conditions,[11-12] AFM can operate under room temperature or 37 °C, in ambient or near-physiological media, thus providing more biologically relevant views at molecular level.

By label-free, local and direct visualization of proteins at the molecular level, we are able to provide unambiguous proof of the binding between COMP and multiple BMP-2 molecules, the conformational information before and after protein complexation, as well as varieties of binding complexes formed in the same mixture. In conjunction with in vitro and in vivo assays, the results could provide new and molecular level insight of how COMP presents BMP-2 molecules to osteoprogenitor cells and enhances osteogenesis. This work is also of translational importance, as the outcome may enable usage of lower BMP-2 dosage for bone repair and regeneration.

2. EXPERIMENTAL

2.1 Materials Used for This Investigation. Dulbecco's modified eagle medium (DMEM), fetal bovine serum (FBS), hydrochloric acid (36.5% to 38.0% w/w), and HEPES (1M) were ordered from Thermo Fisher Scientific (Hampton, NH). Eagle's Minimum Essential Media was purchased from ATCC and phosphate-buffered saline (PBS) (1X) were purchased from Mediatech (Manassas, VA). Hygromycin was ordered from Calbiochem (La Jolla, CA). Sodium chloride (≥99%), calcium chloride (≥96%), dexamethasone (≥97%), β-glycerophosphate disodium salt hydrate (≥99%), L-ascorbic acid (99%), alizarin red stain (pH 4), cetylpyridinium chloride, and glycerol (≥99.5%) were all purchased from Sigma-Aldrich (St. Louis, MO). Microplate of 96-well plates and neolite reagent were ordered from Perkin-Elmer (Waltham, MA). Deionized water with a resistivity of 18.2 MΩ•cm was generated using a Millipore MilliQ system (EMD Millipore, Billerica, MA). Powder 11-mercapto-1-undecanal disulfide $[-S(CH_2)_{10}CHO]_2$ was purchased from

ProChimia (Gdansk, Poland). Acetic acid glacial and 200 proof pure ethanol were purchased from VWR (King of Prussia, PA).

2.2 Expression of Recombinant Protein. The expression and purification of recombinant human COMP was described previously.[5] Briefly, the COMP expression cassette was cloned into a pCCL3 lentiviral vector and stably transfected into human 293T cells. Recombinant human COMP was purified from serum-free cell culture medium by nickel-NTA column affinity chromatography. Purified COMP was dialyzed with 20 mM HEPES buffer (pH 7.8), 500 mM NaCl, 2 mM $CaCl_2$ and 30% glycerol was added before storing at -80 °C. Clinical grade recombinant human BMP-2 was purchased in the form of INFUSE® Bone Graft (Medtronic, Memphis, TN) with a molecular weight of approximately 26 kDa. The lyophilized BMP-2 was resuspended in 20 mM acetic acid or 4 mM hydrochloric acid to a working concentration of 7700 nM.

2.3 Cell Culture. C2C12 mouse myoblast cells were maintained in proliferation medium containing Dulbecco's modified medium (DMEM) and 10% v/v heat-inactivated FBS. The medium was changed every 3 days. Human cervical carcinoma cells with a BMP responsive element, C33A-2D2 cells were given as a gift from Dr. Martine Roussel, and described previously.[13] The parental C33A cells were purchased from ATCC. C33A-2D2 cells were cultured in Eagle's Minimum Essential Media (EMEM) with 10% FBS and 0.38 mM hygromycin.

2.4 Luciferase Assay for Transcriptional Activation. C33A-2D2 cells were expanded in EMEM with 10% FBS and 0.38 mM hygromycin for selective pressure. Cells were seeded at 20,000 cells per well in opaque white 96-well plates in phenol red and glutamine-free EMEM with addition of 2 nM BMP-2 and/or 2 nM COMP. COMP and BMP-2 were incubated together for 20-30 minutes at room temperature before addition to culture media. After 19 hours, neolite reagent

was used according to manufacturer's instructions. Luciferase-substrate light production was quantified in a 96-well Microlumat Plus LB 96V luminometer (Berthold Technologies, Oak Ridge, TN).

2.5 Alkaline Phosphatase Activity. Alkaline phosphatase was measured to indicate markers of osteogenic lineage and predict future matrix mineralization. C2C12 cells were seeded at 1000 cells/cm^2 in a 6-well plate and incubated for 24 hours. Then, the medium was replaced with osteogenic media (DMEM supplemented with 10% FBS, 100 nM dexamethasone, 0.28 mM ascorbic acid, 10 mM β-glycerophosphate, and 2 nM BMP-2 and/or 0.4 nM COMP). After 7 days, alkaline phosphatase activity in the cell lysates was measured using a Sensolyte kit according to kit instructions (Anaspec, Fremont, CA). Briefly, cells were washed with assay buffer and then gently rocked in assay buffer mixed with Triton-X to dislodge the cells. Cells were then vortexed prior to centrifugation at 2500 xg for 10 minutes to pellet cell debris. Supernatant was collected and alkaline phosphatase absorbance at 405 nm was measured by microplate reader. Total supernatant protein was determined by detergent compatible Bradford assay (Fisher Scientific, Hampton, NH).

2.6 Alizarin Red Stain for Matrix Mineralization. C2C12 cells were grown in DMEM medium with 10% FBS, 0.28 mM ascorbic acid, and 10 mM β-glycerophosphate with addition of 2 nM BMP-2 and/or 0.4 nM COMP. Alizarin red staining was performed at 21 days to qualitatively assess matrix mineralization as previously described.[3] Briefly, media was aspirated, and wells were washed 3 times with de-ionized water. Cells were fixed in 70% of ethanol for one hour, then stained with 40 mM alizarin red stain (pH 4.2) for 10 minutes with agitation. Cells were imaged on a Nikon TE200 inverted optical microscope. Mineral density was quantified by extracting the

stain with 10% (w/v) cetylpyridine solution in 10 mM phosphate buffer, pH 7.0, and reading the absorbance at 570 nm.[14]

2.7 Protein Immobilization on Mica(0001) Surface. COMP stock solution (670-950 nM) and BMP-2 stock solution (7700 nM) were diluted to the desired working concentration (2 nM for COMP and 2 nM for BMP-2) with 20 mM HEPES buffer, pH 7.0, with 100 mM NaCl and 2 mM $CaCl_2$. 100 µl of 2 nM COMP was deposited on freshly cleaved mica(0001) surface for 2 minutes. [8, 15] The mica(0001) surface was washed with ultra-pure Milli-Q water (18.2 MΩ.cm) to remove unbound proteins and buffer components. The mica(0001) surface was dried with compressed air, and the sample was imaged immediately after preparation.

For the BMP-2/COMP mixture, 2 nM of BMP-2 and 2 nM of COMP were pre-mixed for 30 minutes at room temperature before deposition, to allow time for complex formation. A volume of 100 µl of BMP-2 and COMP mixture were deposited onto a freshly cleaved mica(0001) surface. After 2 minutes, the surface was gently washed with ultra-pure Milli-Q water (18.2 MΩ.cm) to remove non-bound proteins and dried with compressed air prior to AFM imaging. Samples were imaged immediately after preparation.

2.8 Protein Immobilization on $CHO(CH_2)_{10}S$/Au Surface. Ultraflat thin gold films, 1500 Å in thickness, were prepared according to the reported procedure.[16] Thiol self-assembled monolayers (SAMs) were prepared by immersing the thin gold films into 0.1 mM thiol solution for at least 24 h.[17] To immobilize proteins, SAMs with an aldehyde-terminated functionality were immersed in the desired protein solution for 5 minutes. The concentration of COMP was 2 nM in 0.2X PBS (pH 7.4). After incubation, the sample was removed from the protein solution and gently washed three times with ultra-pure Milli-Q water (18.2 MΩ.cm) before AFM imaging in buffered solution.

2.9 Atomic Force Microscopy. Atomic force microscopy (AFM) images were taken with Asylum Research MFP-3D AFM (Oxford instrument, Santa Barbara, California, U.S.A.). All images of proteins immobilized on mica(0001) were acquired using an MSNL cantilever (k = 0.6 N/m, Olympus, U.S.A.) in tapping mode in air. The driving frequency of the cantilever was typically 109 kHz, the free amplitude was 0.25-0.40 V, and the damping amplitude ranged 22 to 50%. AFM images of COMP immobilized on aldehyde-terminated SAM were taken with an MSNL cantilever (k = 0.6 N/m, Olympus, U.S.A.) in buffer solution. The driving frequency was in resonance with the fundamental vibration of the cantilever, typically 37 kHz in water. All images were taken with a 0.5 x 0.5 μm^2 scan area. Images were acquired at speeds of 1-10 $\mu m\ s^{-1}$, with 1024 x 512 pixels per frame. Data acquisition were carried out using MFP-3D software developed based on Igor Pro 6.12 platform. Typically, at least 5 images were acquired for each experiment. Using tapping mode and soft cantilevers (e.g. k = 0.6 N/m) under ambient conditions, and especially in buffer media were known to exhibit little perturbation to immobilized protein molecules on surfaces.[18-22] For imaging display and analysis, MFP-3D software were utilized, in conjunction with WSXM and ImageJ.

3. RESULTS AND DISCUSSION

3.1 Functional Validation of COMP, BMP-2, and Their Complexes. Before performing high-resolution AFM imaging, it was critical to check and verify that purified proteins retained their biological activity. To this end, we adopted well-accepted in-vitro assays for osteogenesis, including a luciferase reporter assay for BMP activity, alkaline phosphatase assay, and matrix mineralization.[23-24] Results from each assay are shown in Figure 1.

First, we determined whether COMP and BMP-2 mixture affected the transcription of BMP-2 response genes by using a luciferase reporter construct driven by the BMP response elements. Similar to prior work, COMP alone had no effect, and BMP-2 up-regulated the luciferase activity, as revealed in Figure 1, top. The mixture of COMP and BMP-2 exhibits an even higher activity than BMP-2 alone. These results indicate that COMP and BMP-2 mixture enhances BMP-2 dependent transcription, which is consistent with previous reports.[3] Detection of luciferase activity is one of the earliest indication of osteogenesis. Therefore, the addition of COMP enhances BMP-2 osteogenesis potential at the initial stage.

We next verified that purified COMP proteins retain their biological activity in enhancing BMP-2 dependent osteogenic differentiation of osteoprogenitor C2C12 cells.[25] Alkaline phosphatase activity is used as a molecular marker of BMP-2 induced osteogenesis at the early stage of osteogenic differentiation. The alkaline phosphate activity of C2C12 cells was measured after 7 days. Our results indicated that COMP showed lower activity than control (basal media) and BMP-2 alone showed enhancement in activity, whereas the mixture of BMP-2 and COMP nearly doubled the enhancement of BMP-2 alone in alkaline phosphatase activity (Figure 1, middle). COMP alone fails to elicit an osteogenic response but enhances the response in the presence of BMP-2, which is consistent with prior studies.[3, 25] Therefore, BMP-2 and COMP mixture is more effective in promoting BMP-2-induced osteogenic activity than BMP-2 alone even at the early stage of osteogenesis.

Matrix mineralization, a late stage hallmark of BMP-2 induced osteogenic differentiation, was measured by alizarin red stain at day 21 (Figure 1, bottom). The results from the alizarin red assays were consistent with the alkaline phosphatase results described above. As expected, control and COMP alone showed low level of matrix mineralization. Mineralization was induced

by BMP-2 alone, and the effect was further enhanced in the presence of COMP and BMP-2 mixture. Adding COMP augments BMP-2 osteogenesis potential even at the late stage of osteogenesis. In addition, it indicates that the biological activity remains active until the late stage of osteogenic differentiation. These results altogether demonstrate the osteogenesis potency as well as the viability of our proteins.

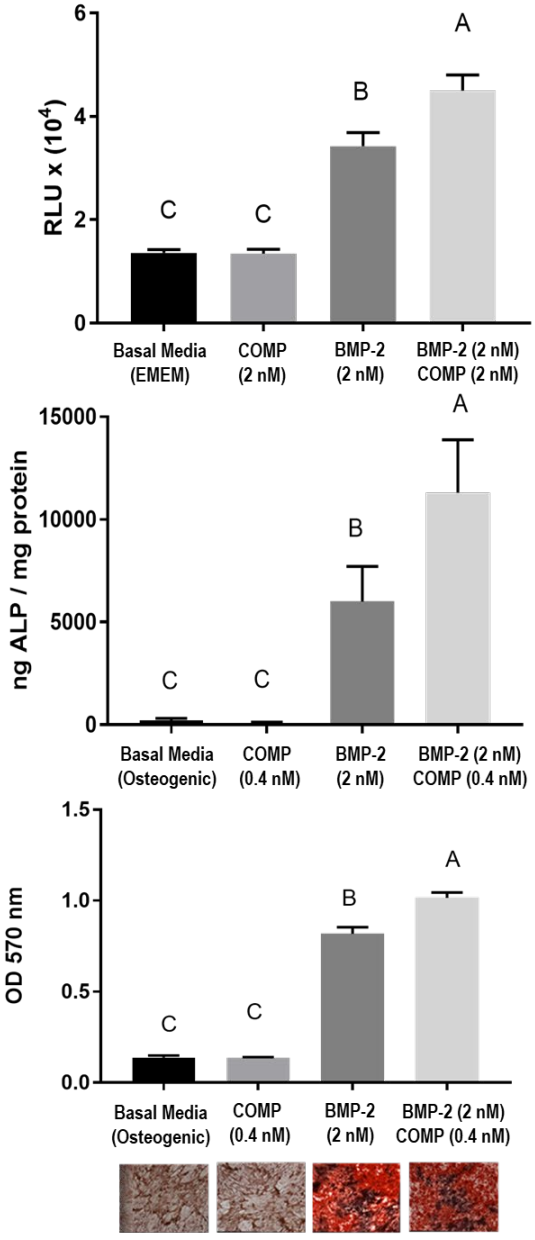

Figure 1. Mixture of COMP and BMP-2 enhanced BMP-2 dependent transcriptional activity and osteogenesis. (Top) Mixture of COMP and BMP-2 enhanced the luciferase activity from a BMP-responsive promoter in C33A-2D2 cells at day 1 (n = 4 technical replicates). (Middle) Mixture of COMP and BMP-2 enhanced the osteogenic alkaline phosphatase activity in C2C12 cells at day 7 (n = 3 technical replicates). (Bottom) Mixture of COMP enhanced BMP-2 dependent matrix mineralization in C2C12 cells measured by alizarin red staining on day 21; the top panels show semi-quantitative assessment of dye amount, and the bottom panels show stained cells (n = 3 technical replicates). Error bars represent the SD via ANOVA with Tukey's HSD and significance set at $p < 0.05$.

3.2 High-Resolution Imaging of COMP Molecules Immobilized on Mica(0001). Individual molecules and intramolecular features of COMP were resolved via AFM as shown in Figure 2. Since mica(0001) is atomically flat, the contrast revealed in Figure 2a is dominated by COMP immobilized on mica(0001). At the scan area of 500x500 nm^2, the orientation, morphology, and intramolecular structures of each COMP can be clearly visualized. Our results reveal the molecular morphology of COMP as a pentameric protein whose five identical units are bundled together with a globular domain at the distal end, manifesting a bouquet-like geometry resembling to a "gecko's foot". COMP is a disulfide-bonded pentameric protein (524 kDa) found in the ECM of cartilage, ligaments, and tendon as well as the vascular smooth muscle.[5, 26-28] The structure of COMP is composed of five identical monomers, each with the following tertiary structure: an amino-terminus that forms disulfide-linked pentamers, four type-2 epidermal growth factor repeat domains, eight type-3 thrombospondin-like domains and carboxyl-terminal "COMP" domain.[27, 29]

X-ray crystallography revealed that the N-termini of pentameric COMP is bundled at the center, with a C-termini domain at the end composing of 15 antiparallel β-strands.[30-32] Our fully stretched "gecko's foot" morphology, Figure 2b, is consistent with the known structure revealed by previous investigations.[5, 33-34]

In addition to the well-known morphology shown in Figure 2b, these intramolecular structures seem to vary from one individual COMP molecule to another, as shown in Figure 2a. Individual protein molecules are known to adopt various orientations upon immobilization on surfaces, e.g. the ellipsoidal shaped BSA could adopt "head-down" or "belly-down" orientation.[17, 20, 35-38] Similarly, in the case of COMP, the "gecko's foot" exhibit various orientations (Figure 2a). More importantly, various intramolecular features, due to the positions of the 5 monomers within each COMP, could be resolved, and those conformations differ from those in Figure 2b. The variation in intramolecular features and conformations upon immobilization are only present for large protein molecules, such as COMP. As shown in Figure 2b-e, COMP could appear in four representative conformations: fully stretched and spread out, with relaxed ends, with buckled anchoring, and with three finger closely packed conformations. The variations of intramolecular features provide corroborating evidence to prior claims that the residues connect N-terminal, and that the arms of COMP monomers are flexible.[5, 33-34] The results shown in Figure 2 are highly reproducible among all of our 8 independent experiments. The robustness was also verified by imaging COMP molecules in buffer upon immobilization on aldehyde-terminated self-assembled monolayers of $CHO(CH_2)_{10}S/Au$.

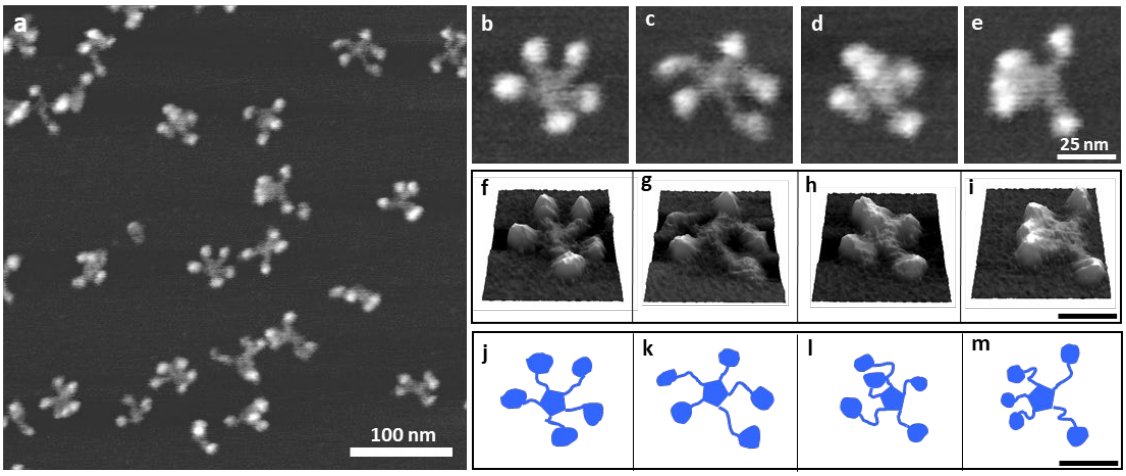

Figure 2. Topographical AFM images of COMP molecules. (a) 0.5 µm x 0.5 µm AFM topographic image of COMP molecules on a freshly cleaved mica(0001) surface. (b-e) Zoomed-in images of four representative conformations of COMP molecules. (f-i) 3D rendered display of the corresponding topographical images. The vertical scale is 2.7 nm. (j-m) Schematics of the four representative conformations of COMP molecules on mica(0001).

Prior X-ray diffraction of a truncated COMP were used in the assignment of the C-terminal and N-terminal. X-ray diffraction of a truncated COMP monomer (EGF4-C-terminal) indicated that the C-terminal extend outward, while the EGF domains are located at the center.[30] However X-ray diffraction of another truncated COMP pentamer (each monomer contains 46 residues from the N-terminal to the arm) indicated that the N-termini are bundled together via disulfide linkage and extend the five arms.[31-32] Piecing the two truncated protein structures together and assuming 5 identical unit, one could infer that the five N-termini bundle at the center of COMP, extending the 5 arms to the C-termini, i.e. the five globular domains. Prior transmission electron microscopy (TEM) images followed the same assignment for the fully stretched pentameric COMP where the arms appeared narrower than the termini.[5, 33-34] Our AFM images revealed various conformations, including the fully stretch pentameric COMP referred to as "Gecko's foot" conformation. The

heights of the C-termini and arm measure 1.9 ± 0.2 nm (n = 20) and 0.8 ± 0.2 nm (n = 15), respectively, as illustrated by the height cursor profiles in Figure 3. These height measurements of C-terminal versus arm remain valid and consistent regardless of the conformation. In the fully stretched conformation, the monomer unit measures 26 ± 4 nm long, which is also consistent with TEM imaging reported previously.[33-34]

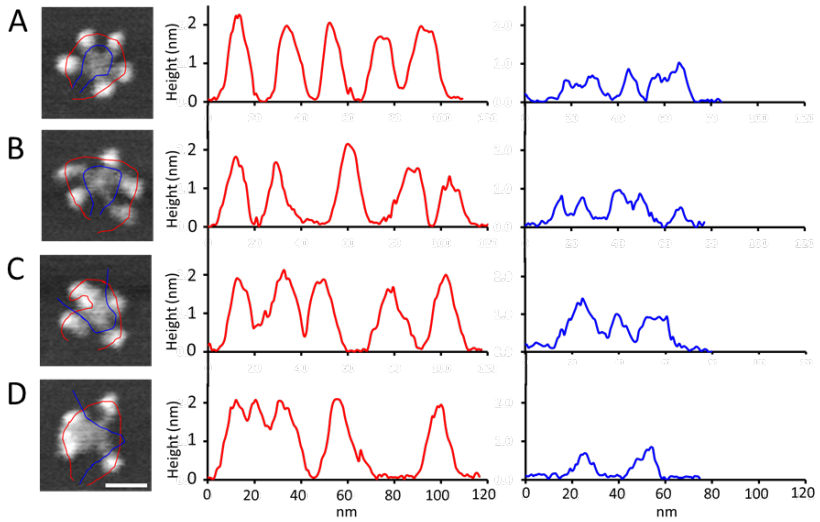

Figure 3. Topographical AFM images and height cursor profile of COMP molecules. (A-D) Topographic AFM images of four representation conformations of COMP molecules on mica(0001) with the corresponding height profile of the C-terminal domains (red) and arms (blue). Scale bar is 25 nm.

3.3 Investigations of COMP and BMP-2 Binding via High-Resolution Imaging. With high resolution AFM images of COMP at hand, we investigated the BMP-2 and COMP interactions by comparing high-resolution studies of COMP and BMP-2 alone and their mixture after immobilization onto mica(0001) surfaces, as shown in Figure 4. Because BMP-2 is much smaller (lateral dimension of 16.8 ± 1.7 nm) than COMP (lateral dimension of 49.7 ± 0.9 nm), a comparison of the mixture (Figure 4C) and COMP (Figure 4A) provides direct evidence that

BMP-2/COMP complex formation occurs. The mixing of BMP-2 and COMP yielded "gummy bear"- shaped molecules, as shown in Figure 4C. This geometry significantly differed from those of COMP (gecko's foot) or BMP-2 (hat), which suggests the occurrence of binding among BMP-2 and COMP, in other words, the formation of complexes. These observations are reproducible, and the protein complexes adopt the same "gummy bear" geometry regardless of reaction media, e.g. from MES (pH 5.5), HEPES (pH 7.0) to PBS (pH 7.4) buffers.

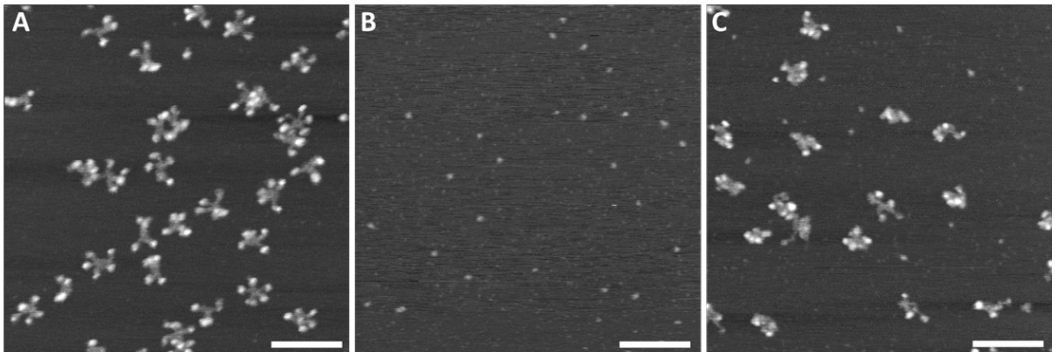

Figure 4. (A) 0.5 μm x 0.5 μm AFM topographic images of COMP molecules immobilized on a mica(0001) surface. (B) Same imaging conditions acquired for BMP-2 molecules on a mica(0001) surface. (C) Same imaging conditions acquired for BMP-2 and COMP mixture immobilized on a mica(0001) surface. Scale bars are 100 nm.

Zoom-in views of these protein complexes, shown in Figure 5, reveal that the "gummy bear" conformation in the BMP-2/COMP complexes have a much more compacted structure than the "gecko's foot" COMP. In the case of COMP with the "gecko's foot" conformation, e.g. in Figure 2b, the spacing between each monomer unit of COMP is clearly evident, in contrast to the pentavalent 5BMP-2/COMP complex, e.g. in Figure 5h. To simply quantify the compactness of COMP and BMP-2/COMP complex, the ratio between the occupied versus the total footprint area of the molecules was measured from AFM topography. The "gecko-foot" COMP measured 65%

(Figure 5a), which is lower than that of penta-valent 5BMP-2/COMP complexes (Figure 5h), 87%. The structure and compactness reveal that COMP provides a relatively stable and ridged presentation of 5 BMP-2, which could mechanistically explain the benefit of sustained BMP-2 signaling and enhanced osteogenic activity of the BMP-2/COMP complex.

Figure 5 illustrates how we identified the number of BMP-2 proteins in each BMP-2/COMP complex. The morphology of COMP molecules used before and after mixing is shown in Figures 5a and 5b, respectively. The molar ratio of BMP-2 to COMP was 1 to 1 (2 nM each protein) which suggest that COMP binding sites are not saturated and there can be COMP molecules with unbound BMP-2 in the mixture. Few conformational changes were observed for COMP molecules without BMP-2 binding. On the basis of analysis of AFM topographic of COMP molecules, the apparent height of the C-termini among COMP molecules measures 1.9 ± 0.2 nm, while the flexible arms of each monomer had an apparent height of 0.8 ± 0.2 nm. In contrast to the COMP geometry, the globular bumps corresponding to the C-terminal domains are no longer present in the "gummy bear" shaped BMP-2/COMP complexes. Instead, the BMP-2/COMP complexes exhibited a more compact structure with many small "bumps" within, as shown in Figure 5 (right two columns). The apparent disappearance of C-terminal bumps is consistent with the flattening of C-terminal domains, as illustrated in the schematic diagram in Figure 5. Prior work suggests the C-terminal domains of COMP as the binding site for ECM components such as collagens[39], fibronectins[40], and growth factors.[5, 27] Previous studies, using truncated COMP protein monomers and BMP-2, also indicated that binding occurred in the C-terminal regions.[26] Our work revealed important new insight, i.e. the C-termini provide binding sites for BMP-2 molecules upon changing of conformation, e.g. flattening. Because the other domains of COMP remained unchanged despite of BMP-2 binding, we infer that the BMP-2

binding would manifest to “bumps” whose heights fall between the 2 thresholds: below the COMP’s C-termini and above the monomer arms. As such, we have counted the numbers of BMP-2 molecule in each of the four complexes as indicated in Figure 5 (c-d,g-h, with arrows), which represent BMP-2/COMP, with 2, 3, 4, 5 BMP-2 molecules (indicated with arrows), respectively. The heterogeneity of multivalent binding in the same protein mixture explains in part the difficulties in generating crystals for BMP-2/COMP complexes. In the case of penta-valency, one COMP bound with five BMP-2 molecules, the compactness reaches 87%, i.e., the complex is relatively ridged and very stable.

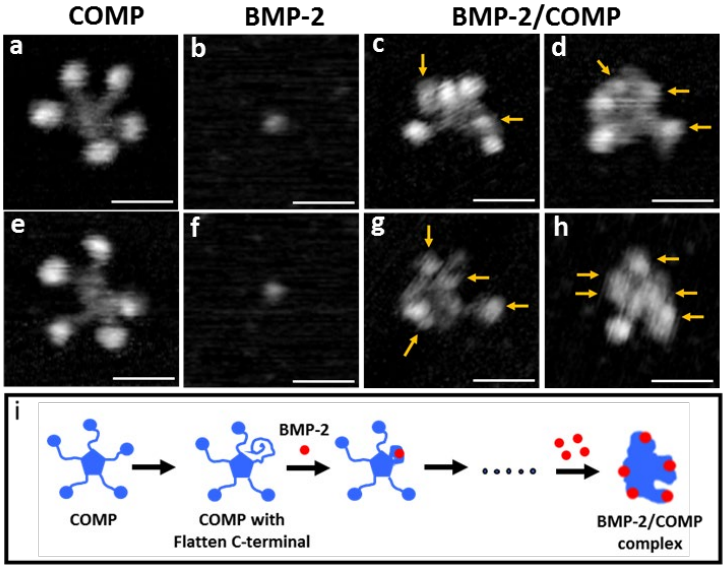

Figure 5. Zoom-in topographical AFM images of COMP, BMP-2 molecules and BMP-2/COMP complexes. (a and e) topographical images of COMP molecules. (b and f) images of BMP-2 molecules. (c,d,g,h) BMP-2/COMP complexes with different number of BMP-2 molecules. Yellow arrows indicate BMP-2 molecules bound to COMP in the complex. Bottom: The schematic diagram illustrates BMP-2 and COMP binding involve conformation changes of COMP, and the final complex exhibits a different geometry, more compact, and lower flexibility than COMP alone. Scale bars are 25 nm.

DISCUSSION

It is known that soluble individual BMP-2 molecules exist as a homodimers, and each BMP-2 interacts with membrane receptors in a divalent manner.[41] This binding event activates the BMP-2 mediated signaling cascade by binding to type-1 and type-2 serine/threonine kinase as illustrated in Figure 6A.[42-44] This work reveals the pentavalency and the conformation of BMP-2/COMP complexes via high-resolution imaging. In addition, our results indicate the reduced flexibility of COMP monomer arms upon binding of BMP-2, as well as the overall change of geometry and conformation. These new insights collectively support the following enhancement mechanism: each BMP-2/COMP complex presents 5 BMP-2 molecules to the receptors in C2C12 membrane at the same time and in close vicinity. On the basis of on our AFM images, the nearest neighbor separation among BMP-2s in the complex ranges from 4-28 nm. Pentavalent presentation of BMP-2 by COMP is equivalent to increasing the local concentration of BMP-2 and reducing ligand mobility (in comparison to the soluble BMP-2), causing clustering of growth factors at the membrane receptors region, thus enhancing the Smad pathway, as shown in Figure 6. In addition, the complexes exhibit stable and higher rigidity structure in comparison to soluble BMP-2 or COMP molecules. These stable and multivalent presentations may increase the binding probability and stability of BMP-2 molecules to the receptor, thus providing sustained activation of BMP-dependent Smad signaling, as shown in Figure 6B.

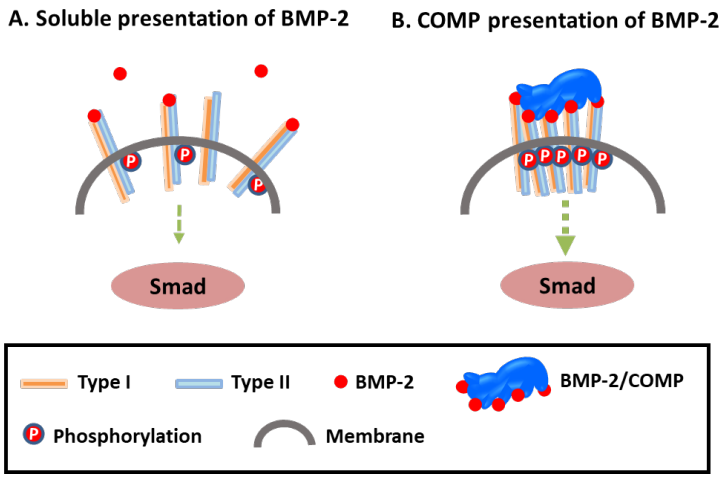

Figure 6. Schematic diagram illustrates the differences between five soluble BMP-2 molecules (A) versus 5-BMP-2/COMP complexes (B) in the context of activated and sustained Smad pathways and eventual osteogenesis.

CONCLUSIONS

This work presents the first direct evidence of multivalent binding between BMP-2 and COMP using AFM imaging. Taking advantages of AFM's high spatial resolution, label-free nature, and high versatility, we first revealed the morphology of COMP molecules: each exhibits a pentameric structure with five identical monomer units bundled together at the N-termini, extending out with flexible chain to C-termini, reminiscent of a "gecko's foot". Variation from this extended conformation was observed upon immobilization on mica(0001) surface, which indicates the flexibility of COMP molecules. Upon mixing with BMP-2, binding between COMP and BMP-2 occurred. The number of BMP-2 molecules each COMP binds varied from complex to complex, mono- to pentavalent binding with BMP-2 molecules were observed. The final protein complexes exhibit much less flexibility in comparison to COMP alone, e.g. the 5BMP-2/COMP complex adopts a "gummy bear" conformation with a higher density and

compactness. These observations are consistent with conformational changes at the C-termini, and rearrangement of the overall conformation of COMP upon binding of BMP-2. The molecular level insight provided by this investigation sheds new light on the mechanism of enhancement of the BMP-2/COMP complex on osteogenesis of osteoprogenitor cells, i.e. the multivalent presentation of BMP-2 via the stable and relatively rigid BMP-2/COMP complex can form multiple BMP-2 and cellular receptor bindings in close vicinity. Work is in progress for in situ and time-dependent study of BMP-2 and COMP binding process and the stability of the complex, as well as the optimization of BMP-2 presentation for longer-lasting, sustained activation of BMP-dependent Smad signaling pathways and enhanced osteogenesis downstream. This work is also of translational importance because the high efficacy of BMP-2/COMP complexes suggest that lower dosage of BMP-2 is possible for bone repair and regeneration. This study demonstrates the importance of AFM as a technique for revealing the structural and molecular mechanism through which presentation of BMP-2 by COMP enhances activity, and hence could lead to the development of engineered or synthetic matrix molecules or alternative presentations that can modulate the activity of BMP-2 and other growth factors in TGF family. The enabling aspect of modulating activities of molecules in TGF family has clinical applications reaching far beyond fracture repair.

ACKNOWLEDGMENTS

This work was supported by the National Institutes of Health (R01AR070239), Department of Defense (CDMRP PR142010), and the Gordon and Betty Moore Foundation.

AUTHOR DISCLOSURE STATEMENT

None of authors has competing interests.

REFERENCES

1. Wozney, J. M. The Bone Morphogenetic Protein Family and Osteogenesis. *Mol. Reprod. Dev.* **1992,** *32*, 160-167.
2. Yamaguchi, A.; Ishizuya, T.; Kintou, N.; Wada, Y.; Katagiri, T.; Wozney, J. M.; Rosen, V.; Yoshiki, S. Effects of Bmp-2, Bmp-4, and Bmp-6 on Osteoblastic Differentiation of Bone Marrow-Derived Stromal Cell Lines, St2 and Mc3t3-G2/Pa6. *Biochem. Biophys. Res. Commun.* **1996,** *220*, 366-371.
3. Ishida, K.; Acharya, C.; Christiansen, B. A.; Yik, J. H.; DiCesare, P. E.; Haudenschild, D. R. Cartilage Oligomeric Matrix Protein Enhances Osteogenesis by Directly Binding and Activating Bone Morphogenetic Protein-2. *Bone* **2013,** *55*, 23-35.
4. Epstein, N. E. Pros, Cons, and Costs of Infuse in Spinal Surgery. *Surg Neurol Int.* **2011,** *2*, 10.
5. Haudenschild, D. R.; Hong, E.; Yik, J. H.; Chromy, B.; Morgelin, M.; Snow, K. D.; Acharya, C.; Takada, Y.; Di Cesare, P. E. Enhanced Activity of Transforming Growth Factor Beta1 (Tgf-Beta1) Bound to Cartilage Oligomeric Matrix Protein. *J. Biol. Chem.* **2011,** *286*, 43250-43258.
6. Urist, M. R. Bone: Formation by Autoinduction. *Science* **1965,** *150*, 893-899.
7. Refaat, M.; Klineberg, E. O.; Fong, M. C.; Garcia, T. C.; Leach, J. K.; Haudenschild, D. R. Binding to Comp Reduces the Bmp2 Dose for Spinal Fusion in a Rat Model. *Spine* **2016,** *41*, E829-E836.
8. Viani, M. B.; Pietrasanta, L. I.; Thompson, J. B.; Chand, A.; Gebeshuber, I. C.; Kindt, J. H.; Richter, M.; Hansma, H. G.; Hansma, P. K. Probing Protein-Protein Interactions in Real Time. *Nat. Struct. Biol.* **2000,** *7*, 644-647.

9. Patil, S.; Martinez, N. F.; Lozano, J. R.; Garcia, R. Force Microscopy Imaging of Individual Protein Molecules with Sub-Pico Newton Force Sensitivity. *J. Mol. Recognit.* **2007,** *20*, 516-523.
10. Engel, J.; Furthmayr, H. Electron-Microscopy and Other Physical Methods for the Characterization of Extracellular-Matrix Components - Laminin, Fibronectin, Collagen-Iv, Collagen-Vi, and Proteoglycans. *Methods Enzymol.* **1987,** *145*, 3-78.
11. Sosa, H.; Dias, D. P.; Hoenger, A.; Whittaker, M.; WilsonKubalek, E.; Sablin, E.; Fletterick, R. J.; Vale, R. D.; Milligan, R. A. A Model for the Microtubule-Ncd Motor Protein Complex Obtained by Cryo-Electron Microscopy and Image Analysis. *Cell* **1997,** *90*, 217-224.
12. Adrian, M.; Dubochet, J.; Lepault, J.; Mcdowall, A. W. Cryo-Electron Microscopy of Viruses. *Nature* **1984,** *308*, 32-36.
13. Vrijens, K.; Lin, W. W.; Cui, J.; Farmer, D.; Low, J.; Pronier, E.; Zeng, F. Y.; Shelat, A. A.; Guy, K.; Taylor, M. R.; et al. Identification of Small Molecule Activators of Bmp Signaling. *Plos One* **2013,** *8*, e59045.
14. Maeda, T.; Matsunuma, A.; Kurahashi, I.; Yanagawa, T.; Yoshida, H.; Horiuchi, N. Induction of Osteoblast Differentiation Indices by Statins in Mc3t3-E1 Cells. *J. Cell. Biochem.* **2004,** *92*, 458-471.
15. Bergkvist, M.; Carlsson, J.; Karlsson, T.; Oscarsson, S.; TM-AFM Threshold Analysis of Macromolecular Orientation: A Study of the Ori-Entation of Igg and Ige on Mica Surfaces. *J. Colloid Interface Sci.* **1998,** *206*, 475-481.
16. Hegner, M.; Wagner, P.; Semenza, G. Ultralarge Atomically Flat Template-Stripped Au Surfaces for Scanning Probe Microscopy. *Surf. Sci.* **1993,** *291*, 39-46.

17. Wadu-Mesthrige, K.; Amro, N. A.; Liu, G. Y. Immobilization of Proteins on Self-Assembled Monolayers. *Scanning* **2000,** *22*, 380-388.

18. Siedlecki, C. A.; Marchant, R. E. Atomic Force Microscopy for Characterization of the Biomaterial Interface. *Biomaterials* **1998,** *19*, 441-454.

19. Hansma, P. K.; Cleveland, J. P.; Radmacher, M.; Walters, D. A.; Hillner, P. E.; Bezanilla, M.; Fritz, M.; Vie, D.; Hansma, H. G.; Prater, C. B.; et al. Tapping Mode Atomic-Force Microscopy in Liquids. *Appl. Phys. Lett.* **1994,** *64*, 1738-1740.

20. Hansma, H. G. Atomic Force Microscopy of Biomolecules. *J. Vac. Sci. Technol.* **1996,** *14*, 1390-1394.

21. Fotiadis, D.; Scheuring, S.; Muller, S. A.; Engel, A.; Muller, D. J. Imaging and Manipulation of Biological Structures with the AFM. *Micron* **2002,** *33*, 385-397.

22. Hansma, H. G.; Sinsheimer, R. L.; Groppe, J.; Bruice, T. C.; Elings, V.; Gurley, G.; Bezanilla, M.; Mastrangelo, I. A.; Hough, P. V. C.; Hansma, P. K. Recent Advances in Atomic-Force Microscopy of DNA. *Scanning* **1993,** *15*, 296-299.

23. Yamaguchi, A.; Katagiri, T.; Ikeda, T.; Wozney, J. M.; Rosen, V.; Wang, E. A.; Kahn, A. J.; Suda, T.; Yoshiki, S. Recombinant Human Bone Morphogenetic Protein-2 Stimulates Osteoblastic Maturation and Inhibits Myogenic Differentiation Invitro. *J. Cell Biol.* **1991,** *113*, 681-687.

24. Rawadi, G.; Vayssiere, B.; Dunn, F.; Baron, R.; Roman-Roman, S. Bmp-2 Controls Alkaline Phosphatase Expression and Osteoblast Mineralization by a Wnt Autocrine Loop. *J. Bone Miner. Res.* **2003,** *18*, 1842-1853.

25. Katagiri, T.; Yamaguchi, A.; Komaki, M.; Abe, E.; Takahashi, N.; Ikeda, T.; Rosen, V.; Wozney, J. M.; Fujisawasehara, A.; Suda, T. Bone Morphogenetic Protein-2 Converts the

Differentiation Pathway of C2c12 Myoblasts into the Osteoblast Lineage. *J. Cell Biol.* **1994,** *127*, 1755-1766.

26. Du, Y.; Wang, Y.; Wang, L.; Liu, B.; Tian, Q.; Liu, C. J.; Zhang, T.; Xu, Q.; Zhu, Y.; Ake, O.; et al. Cartilage Oligomeric Matrix Protein Inhibits Vascular Smooth Muscle Calcification by Interacting with Bone Morphogenetic Protein-2. *Circ. Res.* **2011,** *108*, 917-928.
27. Acharya, C.; Yik, J. H.; Kishore, A.; Van Dinh, V.; Di Cesare, P. E.; Haudenschild, D. R. Cartilage Oligomeric Matrix Protein and Its Binding Partners in the Cartilage Extracellular Matrix: Interaction, Regulation and Role in Chondrogenesis. *Matrix Biol.* **2014,** *37*, 102-111.
28. Hedbom, E.; Antonsson, P.; Hjerpe, A.; Aeschlimann, D.; Paulsson, M.; Rosapimentel, E.; Sommarin, Y.; Wendel, M.; Oldberg, A.; Heinegard, D. Cartilage Matrix Proteins - an Acidic Oligomeric Protein (Comp) Detected Only in Cartilage. *J. Biol. Chem.* **1992,** *267*, 6132-6136.
29. Newton, G.; Weremowicz, S.; Morton, C. C.; Copeland, N. G.; Gilbert, D. J.; Jenkins, N. A.; Lawler, J. Characterization of Human and Mouse Cartilage Oligomeric Matrix Protein. *Genomics* **1994,** *24*, 435-439.
30. Tan, K.; Duquette, M.; Joachimiak, A.; Lawler, J. The Crystal Structure of the Signature Domain of Cartilage Oligomeric Matrix Protein: Implications for Collagen, Glycosaminoglycan and Integrin Binding. *FASEB J.* **2009,** *23*, 2490-2501.
31. Malashkevich, V. N.; Kammerer, R. A.; Efimov, V. P.; Schulthess, T.; Engel, J. The Crystal Structure of a Five-Stranded Coiled Coil in Comp: A Prototype Ion Channel? *Science* **1996,** *274*, 761-765.
32. Efimov, V. P.; Engel, J.; Malashkevich, V. N. Crystallization and Preliminary Crystallographic Study of the Pentamerizing Domain from Cartilage Oligomeric Matrix Protein: A Five-Stranded Alpha-Helical Bundle. *Proteins* **1996,** *24*, 259-262.

33. Dicesare, P. E.; Morgelin, M.; Carlson, C. S.; Pasumarti, S.; Paulsson, M. Cartilage Oligomeric Matrix Protein - Isolation and Characterization from Human Articular-Cartilage. *J. Orthop. Res.* **1995,** *13*, 422-428.

34. Morgelin, M.; Heinegard, D.; Engel, J.; Paulsson, M. Electron-Microscopy of Native Cartilage Oligomeric Matrix Protein Purified from the Swarm Rat Chondrosarcoma Reveals a 5-Armed Structure. *J. Biol. Chem.* **1992,** *267*, 6137-6141.

35. Liu, G. Y.; Amro, N. A. Positioning Protein Molecules on Surfaces: A Nanoengineering Approach to Supramolecular Chemistry. *Proc. Natl. Acad. Sci. U. S. A.* **2002,** *99*, 5165-5170.

36. Tan, Y. H.; Liu, M.; Nolting, B.; Go, J. G.; Gervay-Hague, J.; Liu, G. Y. A Nanoengineering Approach for Investigation and Regulation of Protein Immobilization. *ACS Nano* **2008,** *2*, 2374-2384.

37. Dorn, I. T.; Eschrich, R.; Seemuller, E.; Guckenberger, R.; Tampe, R. High-Resolution Afm-Imaging and Mechanistic Analysis of the 20 S Proteasome. *J. Mol. Biol.* **1999,** *288*, 1027-1036.

38. Yang, J.; Tamm, L. K.; Somlyo, A. P.; Shao, Z. Promises and Problems of Biological Atomic-Force Microscopy. *J. Microsc.* **1993,** *171*, 183-198.

39. Blumbach, K.; Niehoff, A.; Paulsson, M.; Zaucke, F. Ablation of Collagen Ix and Comp Disrupts Epiphyseal Cartilage Architecture. *Matrix Biol.* **2008,** *27*, 306-318.

40. Di Cesare, P. E.; Chen, F. S.; Moergelin, M.; Carlson, C. S.; Leslie, M. P.; Perris, R.; Fang, C. Matrix-Matrix Interaction of Cartilage Oligomeric Matrix Protein and Fibronectin. *Matrix Biol.* **2002,** *21*, 461-470.

41. Scheufler, C.; Sebald, W.; Hulsmeyer, M. Crystal Structure of Human Bone Morphogenetic Protein-2 at 2.7 Angstrom Resolution. *J. Mol. Biol.* **1999,** *287*, 103-115.

42. Derynck, R.; Zhang, Y. E. Smad-Dependent and Smad-Independent Pathways in Tgf-Beta Family Signalling. *Nature* **2003,** *425*, 577-584.
43. Miyazawa, K.; Shinozaki, M.; Hara, T.; Furuya, T.; Miyazono, K. Two Major Smad Pathways in Tgf-Beta Superfamily Signalling. *Genes Cells* **2002,** *7*, 1191-1204.
44. Miyazono, K. Signal Transduction by Bone Morphogenetic Protein Receptors: Functional Roles of Smad Proteins. *Bone* **1999,** *25*, 91-93.

TOC GRAPHIC